AIAA 2001-1588

SRTM ON-ORBIT STRUCTURAL DYNAMICS

Jeffrey W. Umland* and Howard Eisen†

Jet Propulsion Laboratory, California Institute of Technology
4800 Oak Grove Drive, M/S 158-224
Pasadena, California 91109

Abstract

One of SRTM's significant features is the use of a 60-meter long deployable mast that serves to deploy an outboard antenna and creates a stable baseline. The structural dynamic issues associated with a 60-meter mast and large tip mass, i. e. the outboard antenna, deployed from the Shuttle are the focus of this paper. Specific topics covered include on-orbit math model development, loads analysis, ground and on-orbit structural dynamic testing. Additionally, a novel approach towards the reduction of mast on-orbit transient response called "Fly-casting" is developed from first principles, and in-flight performance of this technique is described.

1. Introduction

The Space Radar Topography Mission (SRTM) flew in February 2000 on the space shuttle Endeavor as the primary payload for STS-99. The objective of this joint project between the National Imagery and Mapping Agency (NIMA) and the National Aeronautics and Space Administration (NASA) is to generate a near-global high-resolution database of the earth's topography. This mission made use of Interferometric Synthetic Aperture Radar (ISAR) to digitally survey the Earth's surface from space. The primary product of this 11-day mission is a topographic database of 80% of the Earth's land surface, i. e. most land surfaces between ± 60° latitude. The resulting digital terrain data set provides a significant improvement over currently existing global topography data sets.

1.1 Instrument Overview

The SRTM architecture is based upon the Spaceborne Imaging Radar/X-band Synthetic Aperture Radar (SIR-C/X-SAR) instruments that flew twice on the Space Shuttle Endeavor in 1994, see Jordan et al, 1995. The SIR-C/X-SAR project was a collaborative effort between NASA, which developed SIR-C, and the German and Italian Space Agencies, which developed X-SAR. The SIR-C instrument was two separate SAR's, which operate in the C, and L-bands. The X-SAR instrument operates in the X-band. The combined SIR-C/X-SAR instruments including electronics essentially fill the shuttle payload bay. The primary objective of the SIR-C/X-SAR missions was the radar imaging of select "supersite" targets. SIR-C/X-SAR's secondary objectives, which enabled SRTM, included the demonstration of repeat pass interferometry and scan-SAR. The repeat pass interferometry data is then used to recover the topographical features of the target surveyed. Scan-SAR is a method of beam steering that is employed by SRTM, in the C-band, such that the radar swath width is sufficient to achieve complete mapping coverage in 159 orbits. See Rosen et al for a detailed treatment of Synthetic Aperture Radar Interferometry.

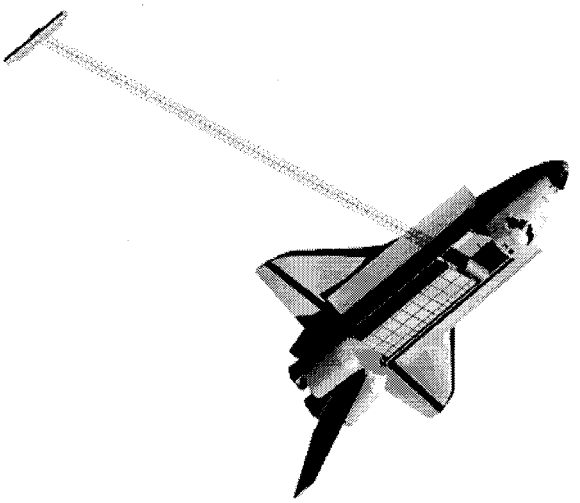

Figure 1. SRTM Mission Configuration

The required modifications to the existing radar instrument to collect the interferometric data included a second C-band antenna, a 60-meter mast, metrology, and additional avionics. Further, the German Space Agency provided a second X-band antenna. The fundamental SRTM instrument configuration is illustrated in figure 1. Simplistically, SRTM makes use of two radar apertures separated by a fixed distance, or baseline, to form a fixed baseline interferometer. The in-board aperture, relative to the Orbiter payload bay, is used to both send and receive radar energy while the outboard antenna only receives energy.

*Senior Engineer, AIAA Member
†Principal Engineer, AIAA Member

1.2 Antenna Mechanical System (AMS)

The original SIR-C/X-SAR instrument is illustrated in figure 2. The weight of the SIR-C/X-SAR instrument is approximately [15,000 lbs]. The top surface of SIR-C/X-SAR, i. e. the C-band panels and L-band panels, is 12 meters by 3.5 meters and is tilted approximately 14 degrees relative to the Orbiter x-y plane. SIR-C/X-SAR's three primary structural mechanical components: a) the Antenna Core Structure (ACS), b) the X-SAR Support Structure (XSS), and c) the Antenna Trunnion Structures (ATS).

The ACS is a conventional bolted/riveted aluminum truss that provides support to the L-band and C-band radar panel arrays. The ACS also provides cabling and waveguide support, and incorporates X-SAR assembly hinge and actuator mounting provisions. The original SIR-C/X-SAR instrument flew one row of 18 C-band panels and 2 rows of 9 L-band panels. SRTM retained the 18 C-band panels, and 6 of the L-band panels. SRTM did not use the L-band panels. The panels are attached pseudo-kinematically to the ACS via four standoffs.

The XSS provides the mounting surface for X-SAR's X-band radar panel arrays. The entire X-SAR assembly, i. e. XSS and panels, is connected only to the ACS and is articulated about the STS x-axis via a tri-drive actuator. X-SAR is launched in a stowed position, which is within the STS payload bay dynamic envelope, and then is rotated about a hinge line to its on-orbit position which exceeds the dynamic envelope.

The ATS is the structure that attaches the ACS to the orbiter. Each of the two ATS's (one forward and one aft) attaches the orbiter in six degrees of freedom, through two sill trunnions, and one keel trunnion. The ACS is then supported on the two ATS's, via a set of linkages, in near statically determinate manner.

Additionally, the SIR-C/X-SAR electronics are stowed on a pallet, which is attached separately to the Shuttle. The weight of the pallet plus electronics is approximately [5,000 lbs].

The additional SRTM hardware added to the SIR-C/X-SAR instrument is illustrated in figure 3. The most significant addition is the Outboard Antenna System (OASYS) and its deployment system. Also shown in figure 3 is the additional metrology and avionics equipment mounted to the AODA Sensor Panel (ASP). Not shown specifically in figure 3 is the AODA Electronics Plate (AEP) mounted on the ACS aft end, and a pair of propellant tanks mounted in the ACS interiors, which are part of an SRTM specific cold gas thruster system. The OASYS is comprised by the a) Outboard Support Structure (OSS), b) outboard C-band panel array, c) outboard X-band panels and electronics, and d) AODA equipment. The OSS is a graphite epoxy and aluminum honeycomb bonded structure which then supports the remaining OASYS equipment. The total weight of the OASYS is 877 lbs.

The OASYS deployment system includes the a) 60-meter mast, b) a mast damping system, c) OASYS fliphinge, and d) an OASYS pitch and yaw attitude adjustment mechanism. The 60-meter deployable truss and its deployment mechanisms are described by Gross and Messner, 1998. The mast damping mechanisms were designed to achieve high, i. e. greater than 10%, damping ratios in the deployed mast first bending modes and the first torsional mode. The OASYS fliphinge rotates the OASYS 180 degrees from its stowed postion to its deployed position once the mast has been deployed. The OASYS pitch and yaw attitude is adjusted via a "warpable" truss called the "Milkstool."

1.3 Attitude and Orbit Determination Avionics (AODA)

The SRTM configuration includes an instrumentation package known as the Attitude and Orbit Determination Avionics (AODA) system, see Duren 1999. AODA provides two fundamental measurements, 1) interferometer baseline measurement and tracking, and 2) SRTM instrument position and attitude reference to inertial space. The interferometer baseline measurement is accomplished via to separate measurements. The baseline length, i. e. distance along the mast, is measured by laser range finders which shoot from the AODA Sensor Panel (ASP) to a corner cube array mounted on the OASYS. The OASYS transverse displacement and attitude is measured by tracking the motion of 3 LED's, mounted to the OASYS, with the ASTRO's Target Tracker (ATT). The ATT is essentially a star tracker that has been refocused to 60 meters. The ATT and LED's are also used during the on-orbit mast structural identification pulse tests, which are described in a following section.

1.4 Selected Mission Design Requirements and Related Structural Dynamic Issues

The SRTM pointing and minimum orbital altitude requirements ultimately generated structural dynamic challenges as the SRTM instrument was designed and implemented. The structural dynamic challenges are classified into the general areas of vibration, strength, system identification.

1.4.1 Pointing

With respect to instrument pointing, the nominal attitude during data acquisition was to: 1) fly the Orbiter with its tail pointed along the velocity vector, 2) rotate the Orbiter about its roll-axis such that the mast was 45 degrees from the local vertical, and 3) radar radiating surfaces oriented toward the ground. Given the attitude requirement and combined SRTM/Orbiter mass properties, the gravity gradient torque was the dominant disturbance torque to the Shuttle reaction control

system. The Orbiter reaction control system was used to maintain SRTM pointing within a 0.01 deg attitude deadband, and 0.1 deg/sec attitude rate deadband. The Orbiter's Digital Auto-Pilot (DAP) was configured such that the 24 lbf. Vernier Reaction Control System (VRCS) jets were used for attitude control. Based on the attitude control requirements, and configuration versus the disturbance torque applied to the system, the reaction control system generated positive roll commands that resulted in jet firings to counter the gravity gradient torque. As a consequence of these jet firings transient vibrations in the mast were generated. Mast tip motion was not a concern to the operation of the radar as an interferometer provided that the knowledge of the tip motion was acquired. Hence, the ATT and LED's were added to SRTM as a metrology system, which tracked the mast motion. The capability of the ATT to acquire and track the motion of the LED's defined a maximum rate of mast motion that could be tracked, this limit was defined to be 2.36 in/sec (6 cm/sec) at the tip of the mast. Additionally, in order for the ATT to acquire the LED the mast tip rates were required to be less than 0.24 in/sec (6 mm/sec) for ten percent of the time during data acquisition. Therefore a mast vibration damping system was implemented to enable the ATT to acquire and track the mast motion given the vibration environment generated by the attitude control system. The requirement levied on the mast vibration damping system is that the modal damping ratios for the mast's first orthogonal bending modes, and the first torsional mode be greater than ten percent.

As a supplement to the Orbiter reaction control system SRTM implemented a cold gas thruster system, which counter balanced approximately half the gravity gradient torque applied to the combined SRTM/Orbiter system. The cold gas thruster amounted to a single thruster mounted to the tip of the mast, and applied a thrust of 0.020 lbf. The addition of this SRTM contained thruster system was independent of the Orbiter's propulsion systems. Significant Orbiter propellant margin was gained, by adding the cold gas thruster at the mast tip, since the disturbance torque to the reaction control was substantially reduced.

1.4.2 Orbital Altitude

In order to achieve the required global mapping coverage and accuracy, C-band radar swath width and overlap requirements were derived. Based on these radar performance requirements, and the capability of the existing SIR-C/X-SAR equipment, orbit requirements were derived for the mission including a minimum orbital altitude of 233 km. After an evaluation of mission simulations it was determined that orbital maintenance, or trim, burns would be required to makeup for the altitude loss due to atmospheric drag on the Orbiter and the deployed mast. It was unacceptable, for mapping accuracy, to begin mapping from a suitably high altitude and just allow the altitude to decay naturally. The orbit trim burns were scheduled for approximately once every 24 hours. Further it was expected that the delta-V required for the trim burns would range from 0.5 to 5 ft/s. The orbit trim burns were performed using two of the Orbiter's +X Primary Reaction Control System (PRCS) jets located in the tail. Each of these jets applies 880 lbs thrust to the Orbiter, and combined applies an approximately 7.5 milli-g acceleration to the system. This inertial acceleration combined with the discrete tip mass, and the mast distributed mass creates a bending moment at the mast root which can then result in significant mast longeron loads. Further since the thrust from the PRCS jets is applied almost instantaneously, mast transient response effects must also be considered, which implies that the mast loads are easily doubled relative to those determined from a quasi-static analysis. SRTM employed a novel thruster pulsing technique, called "Fly-casting," in order to minimize the mast transient response during the daily trim burn. In general, the Orbiter jets were pulsed during the trim burn such that a quasi-static response of the mast was realized and the mast transient vibration was minimized.

2. Analysis and Design

The structural dynamic issues that required specific detailed assessment during the development of SRTM were a) Shuttle attitude control system stability, and b) deployed mast loads and structural adequacy. The control system and structural assessments were accomplished via an integrated SRTM and Shuttle structural dynamic math model.

2.1 Mass Properties

The coupled SRTM and Orbiter mass properties are given in table 1. Additionally, the respective separate SRTM and Orbiter mass properties are also given in table 1. These mass properties are given in the Orbiter Structural Reference Frame. While SRTM is roughly ten percent of the mass of the Orbiter, SRTM's roll moment of inertia is (I_{xx}) is twice that of the Orbiter.

2.2 Structural Dynamic Model Development

JPL created an SRTM on-orbit structural dynamic math model, which was then provided to the various organizations within the STS program that perform various structural dynamic analyses. Specifically, Charles Stark Draper Laboratories (CSDL) provided the flight control design and assessment, on-orbit loads support, and procedure development. Boeing North America (BNA) also provided on-orbit loads support. In total, there were three independent organizations performing on-orbit analysis functions, which provided a good check against integrated modeling and analysis errors. Each of the three organizations employed slightly different integrated modeling approaches and

computational environments. For example JPL combined Craig-Bampton substructure math models within a Matlab environment to perform on-orbit loads and dynamic analysis.

The SRTM mast damping system utilized fluid filled damping cartridges, which were then modeled as viscous dampers in the analytical assessments. The complex modal behavior induced by the discrete viscous damping elements was properly captured in the on-orbit coupled loads analysis. The approach taken to here was to provide an SRTM substructure model based on normal modes, e.g. Craig-Bampton mass and stiffness matrices were provided to BNA. The damper attach grid points were retained as interface degrees of freedom in the substructure formulation. Once the respective substructure models were integrated to form the coupled model, a full damping matrix was computed by applying a collocated rate dependent force to the damper interface degrees of freedom. Table two provides a summary of the analytical on-orbit SRTM structural dynamic characteristics, in terms of modal frequency and damping ratios, as well as a comparison of the results as provided by JPL, CSDL, and BNA. The results given in table two assume nominal damper performance.

The mast vibration damping system was comprised of two separate mechanisms see Umland 2001. The bending mode damping mechanism was configured and tuned such that high damping is achieved in the first pair of orthogonal bending modes. Conceptually, the bending mode damping mechanism is a spring a dashpot that are arranged to mechanically operate in parallel. As implemented, the bending mode damper consisted of three hermetically sealed viscous damping cartridges, and three springs. Each viscous damping cartridge was installed concentric with its parallel spring. The torsional mode damping mechanism was similar to the bending mode damper, with the exceptions that the torsion mode damper used only one damping cartridge and a parallel spring was not required. The damping cartridges selected have a small inherent static spring stiffness that is parallel to the damping. Further, the damping cartridges used in the bending mode damper required a significantly higher damping coefficient than the cartridge used in the torsion mode damper. While all the damping cartridges used were mechanically identical, the damping coefficient was adjusted by filling the cartridges with silicone fluid with different viscosity, e. g. the bending mode damping cartridges were filled with 100 cSt silicone fluid, while the torsion mode damping cartridge used 10 cSt silicone fluid. The two mast damping mechanisms were a JPL design, and the damping cartridges were contracted to a vendor that specializes in damper manufacturing.

During the flight control system and on-orbit coupled loads assessments performed for SRTM, the damping mechanism failure modes and the resultant changes in mast modal properties were a primary consideration. Both damping mechanisms were considered to have three specific states, that is a nominal or properly functioning state, and two failed states. The nominal state was defined as the damper "strokes" normally and provides a reaction force that is proportional to the rate that the one cartridge end is displaced relative to the other. The two failure states considered were 1) a "seized" damping mechanism, and 2) a "soft" cartridge, i. e. the fluid had drained out of an individual cartridge. For the purposes of the flight control system design it was assumed that these failures could occur at any time during the mission at that the failure would not be readily detected. One credible scenario of how a damping mechanism could be seized is, if during its operation a foreign object is entrained into the mechanism the mechanism may jam. Great care was taken to preclude such a scenario, yet prudently it was considered credible. The second damper failure mode was the "soft" damper, here the consideration was that somehow the viscous fluid had leaked out of the cartridge. While the cartridges were completely hermetically sealed via weldments, the hermeticity precluded closure weldment leak tests. Additionally, X-ray inspection of the final closure welds proved to be impractical, and inconclusive. Hence the "soft" damper cartridge failure was considered credible. Further, the flight control system and on-orbit loads assessments were conducted with the proviso that the payload shall be two-fault tolerant to credible independent failures. The various damper failure cases, and credibility determination, are given in table three. The corresponding modal characteristics, frequency and damping, for the failure cases defined in table three, are given in table four.

2.3 Flight Control System Design

Notch filters were employed within the Orbiter DAP such that adequate controller stability margins were maintained given the low frequency dynamics of the mast. All credible cases listed in table three were considered as the notch filters were developed. Further, different notch filter sets were developed for different DAP modes, i. e. maneuver versus attitude hold. CSDL is the responsible organization for Orbiter flight control design.

2.4 Fly-Casting

SRTM developed a novel approach towards the reduction of mast member transient response loads during the orbit trim burns. The approach taken was to provide an initial jet pulse and delay immediately prior to the burn such that the mast would then exhibit a quasi-static response during the trim burn. The effect of the initial jet pulse and wait sequence is to cause the

mast to deflect from its unloaded equilibrium position to a new equilibrium deflection that is associated with the rigid body inertial acceleration. In effect the initial pulse and wait causes the mast to deflect and the main pulse catches the mast in a deflected state just at the instant when the mast has zero kinetic energy in the dominant vibration mode.

Consider the simple dynamic system illustrated in figure 4, such a model is intended to represent a rigid body with a flexible appendage. The flexible appendage is represented as a single degree of freedom oscillator attached to the rigid base body. If a force F_t is applied the resultant system acceleration is

$$a = \frac{F_{thrust}}{M_{total}} \tag{1}$$

Several assumptions implicit in equation (1) relative to the simple model are that: a) the appendage mass is small compared to the base body mass, b) rotational effects due center of mass off set are ignored. Therefore, given an Orbiter mass of 235,000 lbm, and a thrust of 1760 lbf, a 7.5 milli-g acceleration will result. The resulting quasi-static appendage relative displacement is then

$$\delta_{tip} = \frac{M_{tip}a}{K_b} \tag{2}$$

Continuing the numerical example, if the equivalent appendage tip mass were 1437 lbm, and the appendage bending stiffness were 0.7 lbf/in, the resulting quasi-static tip displacement would be 15.4 in. Further, due the transient response of the appendage the maximum tip displacement would be twice that of the quasi-static response. Given that the internal appendage loads and stresses are directly related to tip displacement, any reduction in the system transient response provides a reduction to the appendage loads and stresses. Now consider the same simple model given in figure 4, and now apply the thrust profile also shown in the figure. Note that the thrust profile has an initial pulse and delay sequence that precedes the main burn. The pulse and delay sequence is reversed at the end of the main burn. Further, the durations of the pulse and delay periods are considered to be equal. The duration of the main burn may be any length, and is ultimately determined by the burn delta-V requirements. The duration of the pulse and delay is readily determined, for this sample problem, given the following boundary conditions: 1) the appendage is at equilibrium prior to the burn, i. e. the strain and kinetic energies associated with the appendage are zero, and 2) at the end of the pulse and delay sequence the appendage's kinetic is zero, while the appendage strain energy is

$$U = \frac{1}{2K_b}\left(M_{tip}a\right)^2 \tag{3}$$

The pulse and delay duration, t_p, is determined by finding the instant at which the total energy, kinetic plus strain, associated with the appendage, due to the transient response induced by the pulse, is equal to the desired final total energy given in equation 3. Therefore the pulse duration, t_p, is

$$t_p = \frac{T}{6} = \frac{\pi}{3\omega} \tag{4}$$

Where T is the period of oscillation of the appendage, and ω is corresponding natural frequency. The response of the simple system shown in figure 4, due to the fly-cast thrust profile is shown in the lower plot also illustrated in figure 4.

The pulse and delay sequence described above presents benefits in terms of reduced transient response for multiple degree of freedom systems whose response to a given forcing function is dominated by a single mode. This was the case for SRTM. The orbit trim burns were specified to be performed by use of a pair of the Orbiter's +X primary reaction control system (PRCS) jets, which apply a total thrust of 1760 lbf predominately along the Orbiter +X axis. This forcing function produces a mast response that is dominated by the mast's x-y plane (yaw) first bending mode. Preflight analysis showed that the frequency of this mode to be 0.096 Hz, implying that the fly-cast timing parameter, T/6, is 1.736 sec. This timing parameter is further rounded to the nearest even multiple of 80 msec, which is the Orbiter DAP update rate. Hence the fly-cast timing, based on preflight estimates, would be 1.76 sec. A typical fly-cast simulation result is shown in figure 5. These results were for nominal damper operation. Points to note from the simulation are that some cross coupling between x and z-axis response is incurred, as well as some second mode response is evident.

As the adequacy of the fly-cast maneuver was evaluated for SRTM a number of practical concerns required consideration, these issues included: 1) damping mechanism failure modes, 2) Orbiter PRCS jet failure modes and corresponding DAP downmoding behavior, 3) crew procedure and required DAP changes during the burn. The damper failure modes, as described in the previous section, required evaluation for the fly-cast relative to their effect on mast member loads. Here it was seen that the high damping for the normally functioning damping mechanisms, tended to pollute the fly-cast response, i. e. for these cases some additional transient response was observed. Conversely, ideal fly-cast response behavior was observed for failure cases that resulted in low damping, provided that the pulse

timing was chosen appropriately. Jet failures during the fly-cast maneuver were a credible failure mode and required evaluation. If a jet fails to fire during maneuver, the DAP automatically selects the next most efficient jet for a desired maneuver. Given that each PRCS jet has at least one redundant jet, which the DAP would normally select to use. Two jet failures were also determined credible and required evaluation. Several mitigating steps were applied during SRTM in order to reduce the, unlikely, probability that a +X jet would fail to fire during the fly-cast maneuver. During the mission design phase it was observed that the possibility of given PRCS jet failure was greatly reduced if that jet had fired successfully at least four times earlier in the same mission. Hence, during the ascent phase of the STS-99 mission a procedure was executed which required that all four of the +X PRCS jets were pulsed. Further, all fly-cast maneuvers were performed open loop, that is the attitude control was not maintained during the fly-cast, this partially precluded the firing of non +X PRCS jets. Further, all non +X PRCS jets were disabled when the SRTM mast was extended. A procedure was developed to quickly restore the all PRCS jets if necessary. The fly-cast crew procedures were developed and practiced extensively in mission simulations. Further, the fly-cast crew procedures were executed as an evaluation during the STS-93 (Chandra) flight.

3. Model Verification

Structural dynamic math models used in coupled loads analyses typically require some level of verification. Payload math models used in launch and landing coupled loads cycles, for example, are normally required to be verified by modal test when the payload exceeds a certain weight. In the case of SRTM test verification of the on-orbit structural dynamics model was a non-trivial task that ultimately relied on both ground testing, and on-orbit system identification.

3.1 Ground Tests

A number of separate tests were performed to support the verification of the SRTM on-orbit math model. First the original SIR-C/XSAR modal test as reported by Smith and Peng, 1993, provided the verification of the SRTM core structure. Additionally, SRTM performed a supplementary modal test that verified the math models of the additional SRTM equipment in launch configuration, specifically the mast canister and the outboard antenna structure. The two modal tests provided the foundation for the SRTM on-orbit modal, although realistically when compared to the very low frequency mast the SRTM core structure is a rigid structure.

Mast frequency identification tests were performed at several stages during the mast assembly phase at AEC-Able. The tests performed on the mast were primarily free-decay type "twang" tests, i. e. the mast was released from a static deflected condition and allowed to oscillate naturally. A fixed base boundary condition was employed in all mast testing. Additionally, a set of air bearings was used to support the mast during the frequency identification testing. The mast tip displacement was then recorded thru the duration of the test. The mast first mode natural frequency was then determined from this data via a number of complementary methods, 1) period of oscillation, 2) power spectral density evaluation of the time domain response, and 3) time domain realization methods, i. e. ERA. The mast finite element model was then updated on the both on the basis of the frequency identification tests, and mast component level mass measurements. Further, bending and torsional static tests were performed on the mast.

The impedance of the damping cartridges was verified by test at the vendor prior to final delivery, and is discussed in further detail in Umland, 2001.

3.2 On-Orbit Tests

A small number of frequency identification pulse tests were performed on the deployed mast as part of the SRTM on-orbit checkout procedure. The objectives of the tests were to: 1) identify the mast low frequency modes of vibration, such that the adequacy of the DAP notch filter design could be verified; 2) verify the fly-cast T/6 timing parameter; 3) verify the expected structural dynamic response of the fly-cast maneuver under less strenuous conditions.

The first objective was accomplished via several independent pulse tests about the Orbiter roll, pitch and yaw axes. The tests were considered to be low amplitude, since the pulses were from the VRCS (24 lbf) jets and were of short duration, 1.52 sec. Further, the tests were performed with the damping mechanisms both locked and unlocked. The results and evaluation the first set of tests showed modal properties consistent with case 15 of table 4. Further, the frequency identification team concluded that both damping mechanisms were failed to a stiff condition. A recommendation was made that the damping mechanisms should be re-locked, and that the notch filters were adequately designed.

The second on-orbit structural dynamic test objective was met by a series of low and higher impulse pulses from the + X PRCS jets, i. e. the same jets to be used for the fly-cast maneuvers. The low impulse pulse tests were specifically two tests one with pulse duration of 0.400 sec, and the second with pulse duration of 0.800 sec. A preliminary fly-cast timing parameter (T/6) was determined to be 1.76 seconds. During the high impulse pulse test, a pulse of 1.76 seconds was applied to verify that the mast frequency did not change given a high amplitude deflection.

The third on-orbit structural dynamic test objective was also accomplished during the high impulse pulse test, by applying a doublet. A doublet is a degenerative form of a fly-cast, where the long duration main pulse is not performed. The expectation of the doublet test that would then confirm the fly-cast physics is that the residual vibration in the mast at the conclusion of the doublet should be minimal. The doublet test was successful.

The pulse tests were successfully completed, all applicable flight rules were met, SRTM was approved to begin mapping under tight deadband attitude control, and the fly-cast maneuver was authorized to be performed according to the timeline.

4. Fly-Casting in Practice

A total of seven fly-cast trim burns were attempted and completed during the SRTM mission. The fly-cast timing parameter of mast yaw mode period over six was determined experimentally to be 1.76 sec (rounded to the nearest 80 msec). The total delta-V applied ranged from 2.9 to 5.1 fps. The main burn duration ranged from 8.8 to 18 sec. A time history of the mast tip deflection for the first fly-cast burn is illustrated in figure 6. An ideal fly-cast configuration was realized for SRTM in part due to the failure of the mast damping system to generate any damping force, which left the system lightly damped.

5. Summary

Ultimately the SRTM mission was successfully completed, and exceeded its global mapping requirements. This success was not without problems along the way. The damping mechanism failure was overcome in part by the overall robust system design, which in effect shows that the dampers were not a required to meet the mission requirements. This robustness is demonstrated in the adequacy of the notch filters, the ATT's ability to track greater than expect mast tip rate motion, and the fly-cast maneuver was amenable to low damping levels. On the other hand, the system robustness was not known a priori and the benefits of adding damping to this system were evident during the design phase. An investigation into the damping mechanism failure was conducted once the mission was over. The root cause of the damper failures was traced to a damping cartridge seizure, where a pair of bushing, that normally allow the cartridge piston rod to translate freely, were swollen to the point that the piston rod could no longer move.

The cold gas thruster used to offset the gravity gradient torque also failed early in the mission. The nature of this failure was that the cold gas thruster system failed to provide a propulsive force, and hence the Orbiter propellant consumption rate increased due to the apparent disturbance torque increas. The root cause of the cold gas thruster system failure was ultimately traced to a set of burst discs placed in the system. Further, the burst discs ultimately failed because insufficient design margin was retained between the burst pressure and the nominal system operating pressure.

SRTM faced significant structural dynamic challenges successfully. A novel trim burn technique, the fly-cast maneuver, was successfully developed and implemented as a matter of routine. A set of system identification tests were performed on-orbit, with a multi-organization team, such that a closed loop attitude control system, with tight pointing requirements, was implemented in time to meet the mapping timeline. Finally, by overcoming the challenges of flying one of the largest space structures, to date, a historic global mapping data set is provided.

6. Acknowledgments

The effort described in this paper was carried out at the Jet Propulsion Laboratory, California Institute of Technology, under contract with the National Aeronautics and Space Administration.

7. References

R. L. Jordan, B. L. Honeycutt, and M. Werner, "The SIR-C/X-SAR Synthetic Aperture Radar System," *IEEE Transactions on Geoscience and Remote Sensing,* Vol. 33, No. 4, July 1995.

D. Gross, and D. Messner, 1999. "The Able Deployable Articulated Mast – Enabling Technology for the Shuttle Radar Topography Mission," *Proc. of the 33rd Aerospace Mechanisms Symposium,* NASA/CP-1999-209259, Pasadena, CA, pp. 15-30.

R. Duren, et al, 1998. "Metrology, attitude, and orbit determination for spaceborne interferometric synthetic aperture radar," *Proc. of the SPIE*, Aerosense Conference.

P. A. Rosen, et al, 2000. "Synthetic Aperture Radar Interferometry," *Proc. of the IEEE*, Vol. 88, No. 3, pp. 333-382.

K. Smith, and C-Y. Peng, 1993. "SIR-C Antenna Mechanical System Modal Test and Model Correlation Report," Jet Propulsion Laboratory, D-10694.

J. Umland, 2001. "SRTM Mast Damping Subsystem Design, and Failure Investigation," *Proc. of the 35th Aerospace Mechanisms Symposium*, Mountain View, CA.

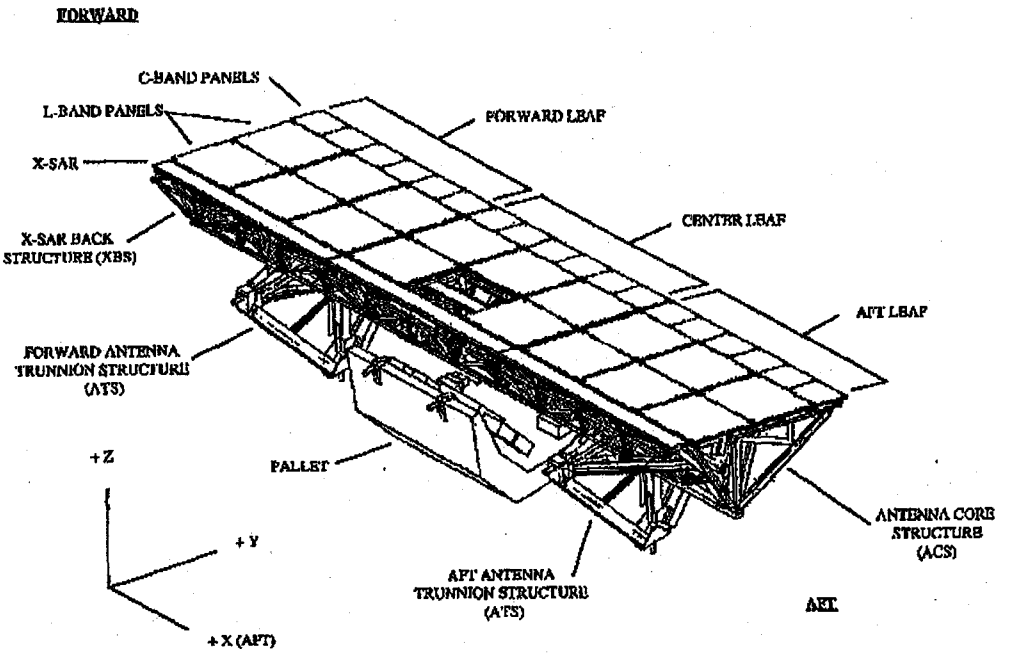

Figure 2. Original SIR-C/X-SAR instrument

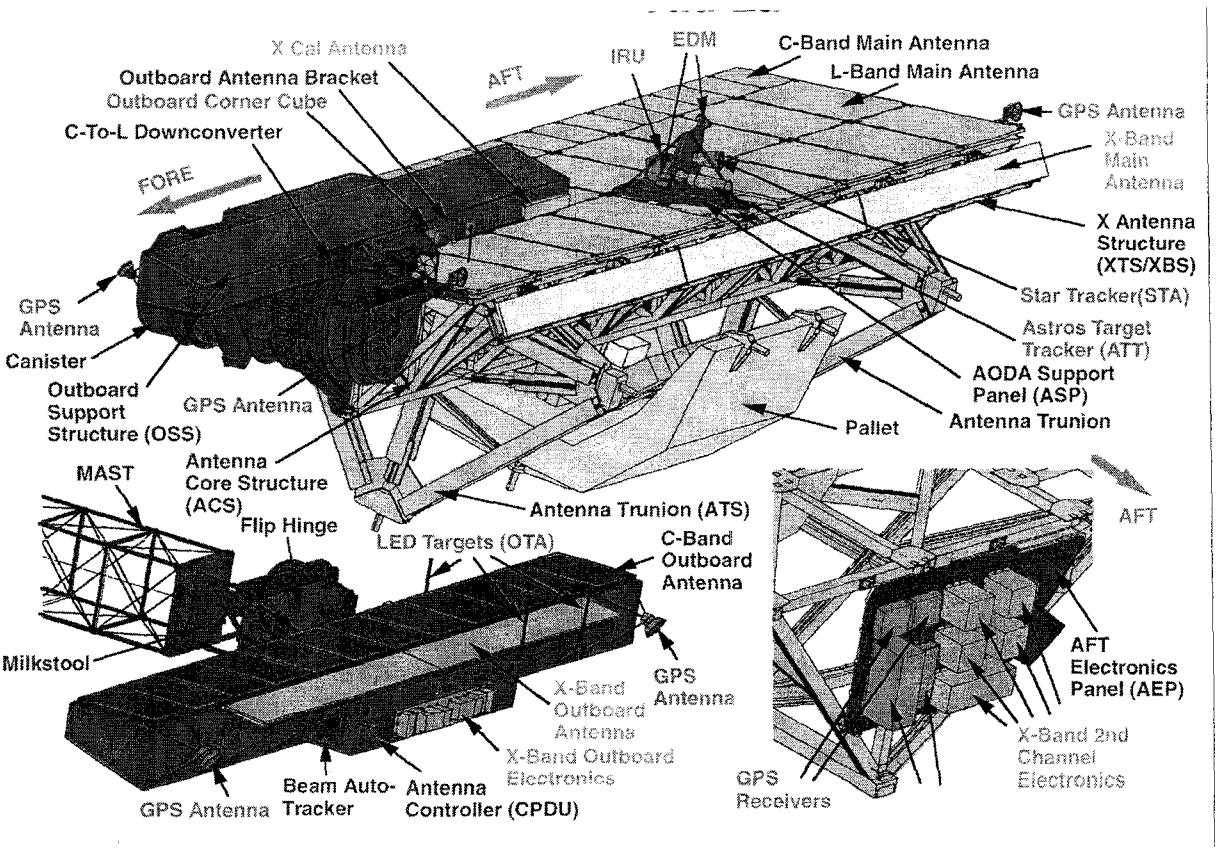

Figure 3. SRTM Instrument, both stowed and deployed configurations

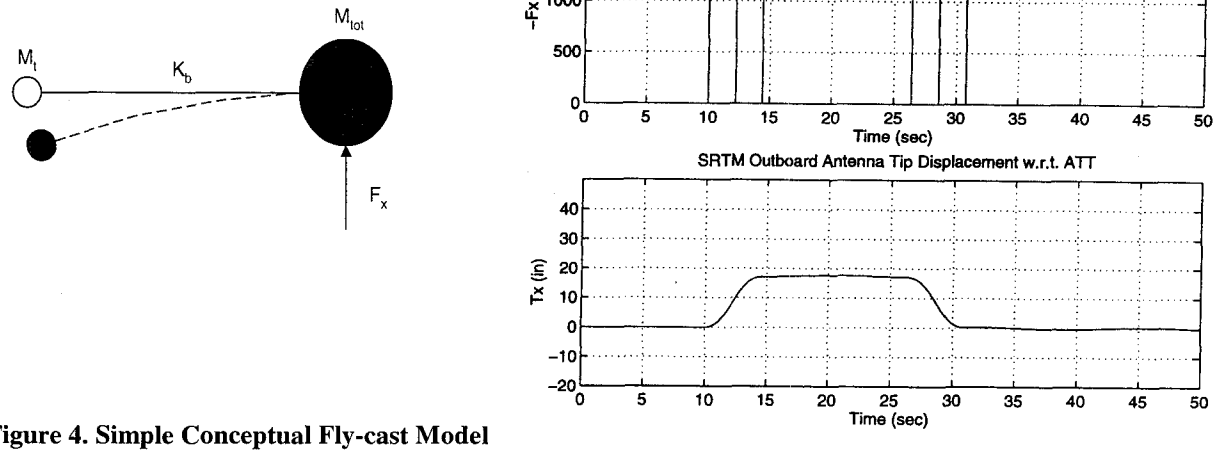

Figure 4. Simple Conceptual Fly-cast Model

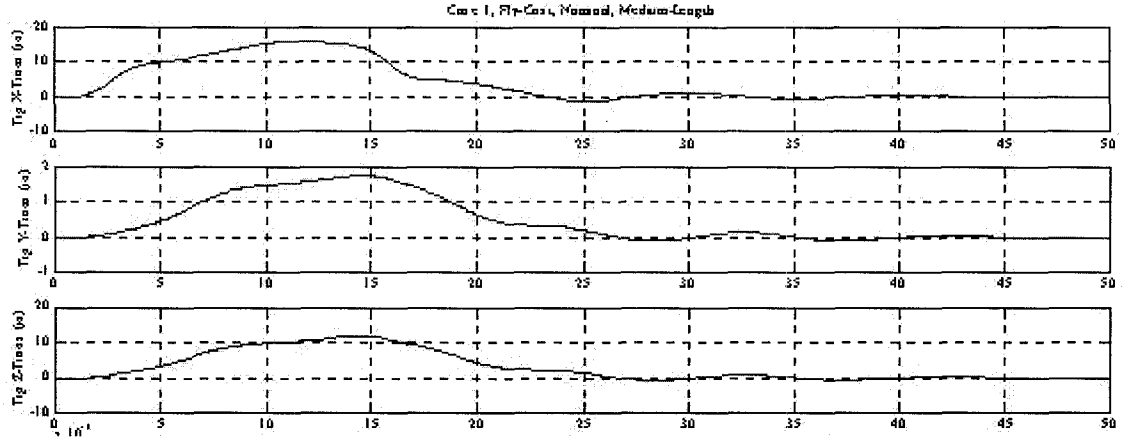

Figure 5. Representative Fly-cast Mast Tip Response with Nominal Damper Operation

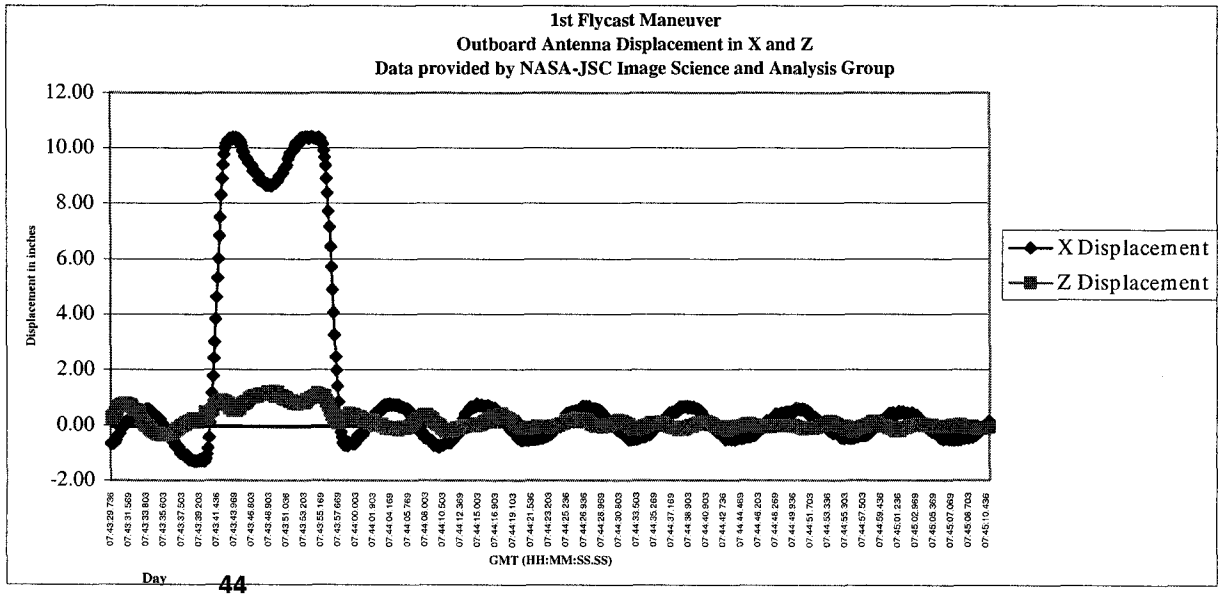

Figure 6. Typical Fly-Cast Burn Time History, Trim Burn #1

Table 1. SRTM Mass Properties

	Deployed SRTM 1/99	Rigid Orbiter w/ Pallet	Orbiter w/ SRTM
Mass (lbm)	21,900	213,391	235,290.
x_{cm} (in)	992.	1097.3	1087.5
y_{cm} (in)	-182.5	-0.6	-17.5
z_{cm} (in)	466.6	372.7	381.5
I_{xx} (10^6 sff)	1.823	0.909	2.912
I_{yy} (10^6 sff)	0.255	7.514	7.854
I_{zz} (10^6 sff)	1.849	7.773	9.811
P_{xy} (sff)	205,678	7,588.	295,301.
P_{xz} (sff)	-54,826	258,700.	161,512.
P_{yz} (sff)	-434,201	66.74	-507,276.

Table 2, Modal Characteristics w/ Nominal Damping

		SRTM w/ Rigid Orbiter		On-Orbit Flex Orbiter		JPL SRTM w/ Flex Orbiter		CSDL SRTM w/ Flex Orbiter		BNA SRTM w/ Flex Orbiter	
Mode Number	Description	ϖ (Hz)	ζ	ϖ (Hz)	ζ	ϖ (Hz)	ζ	ϖ (Hz)	ζ	ϖ (Hz)	ζ
7	Overdamped Local Mode	0.0455	1			0.0456	1	0.047	1	0.0492	1
8	Mast Yaw Bending	0.0963	0.146			0.0971	0.151	0.099	0.150	0.0997	0.148
9	Mast Roll Bending	0.127	0.176			0.125	0.180	0.126	0.194	0.124	0.224
10	Mast Twist	0.188	0.105			0.188	0.110	0.188	0.109	0.188	0.110
11	Overdamped Local Mode	0.300	1			0.295	1	0.297	1	0.299	1
12	Orbiter Payload Bay Door			0.470	0.005	0.473	0.005	0.473	0.005	0.473	0.005
13	Orbiter Payload Bay Door			0.470	0.005	0.477	0.005	0.477	0.005	0.477	0.005
14	Overdamped Local Mode	0.639	1			0.650	1	0.647	1	0.640	1
15	Orbiter Payload Bay Door			0.683	0.005	0.683	0.005	0.683	0.005	0.683	0.005
16	Orbiter Payload Bay Door			0.683	0.005	0.684	0.005	0.684	0.005	0.684	0.005
17	Mast 2nd Bending	0.845	0.061			0.844	0.065	0.851	0.015	0.853	0.016
18	Mast 2nd Bending	0.851	0.010			0.850	0.015	0.855	0.070	0.876	0.077
19	Orbiter Payload Bay Door			1.105	0.005	1.104	0.005	1.104	0.005	1.104	0.005
20	Orbiter Payload Bay Door			1.105	0.005	1.104	0.005	1.104	0.005	1.104	0.005
21	Orbiter Payload Bay Door			1.561	0.005	1.559	0.005	1.559	0.005	1.559	0.005
22	Orbiter Payload Bay Door			1.561	0.005	1.560	0.005	1.560	0.005	1.560	0.005
23	Orbiter Payload Bay Door			1.783	0.005	1.782	0.005	1.782	0.005	1.782	0.005
24	Orbiter Payload Bay Door			1.783	0.005	1.783	0.005	1.782	0.005	1.783	0.005
25	Orbiter Payload Bay Door			1.887	0.005	1.883	0.005	1.883	0.005	1.883	0.005
26	Orbiter Payload Bay Door			1.888	0.005	1.885	0.005	1.884	0.005	1.885	0.005
27	Mast Higher Order Mode	1.987	0.005			1.989	0.005	1.988	0.005	1.989	0.005
28	Mast Higher Order Mode	1.992	0.005			1.992	0.005	1.992	0.005	1.992	0.005
29	Coupled SRTM/Orbiter					2.262	0.007	2.262	0.007	2.261	0.007
30	Mast Higher Order Mode	2.317	0.012			2.315	0.017	2.338	0.018	2.378	0.021
31	Mast Higher Order Mode	2.663	0.005			2.663	0.009	2.664	0.009	2.664	0.009
32	Coupled SRTM/Orbiter					2.954	0.006	2.972	0.006	2.957	0.005
33	Mast Higher Order Mode	3.066	0.005			3.094	0.006	3.113	0.005	3.094	0.005

Table 3, Damper Failure Matrix

Case #	Bending #1	Bending #2	Bending #3	Torsion	Failures	
1	OK	OK	OK	OK	0	Credible
2	**Soft**	OK	OK	OK	1	Credible
3	OK	**Soft**	OK	OK	1	Credible
4	OK	OK	**Soft**	OK	1	Credible
5	OK	**Soft**	**Soft**	OK	2	Credible
6	**Soft**	OK	**Soft**	OK	2	Credible
7	**Soft**	**Soft**	OK	OK	2	Credible
8	OK	OK	OK	**Soft**	1	Credible
9	**Soft**	OK	OK	**Soft**	2	Credible
10	OK	**Soft**	OK	**Soft**	2	Credible
11	OK	OK	**Soft**	**Soft**	2	Credible
12	OK	**Soft**	**Soft**	**Soft**	3	REF
13	**Soft**	OK	**Soft**	**Soft**	3	REF
14	**Soft**	**Soft**	OK	**Soft**	3	REF
15	**Stiff**	**Stiff**	**Stiff**	**Stiff**	2	Credible
16	OK	OK	OK	**Stiff**	1	Credible
17	**Stiff**	**Stiff**	**Stiff**	OK	1	Credible
18	**Soft**	**Soft**	**Soft**	**Soft**	4	REF
19	**Stiff**	**Stiff**	**Stiff**	**Soft**	2	Credible
20	**Soft**	OK	Ok	**Stiff**	2	Credible
21	OK	**Soft**	OK	**Stiff**	2	Credible
22	OK	OK	**Soft**	**Stiff**	2	Credible
23	OK	**Soft**	**Soft**	**Stiff**	3	REF
24	**Soft**	OK	**Soft**	**Stiff**	3	REF
25	**Soft**	**Soft**	Ok	**Stiff**	3	REF
26	**Soft**	**Soft**	**Soft**	**Stiff**	4	REF
27	**Soft**	**Soft**	**Soft**	OK	3	REF

Table 4, Modal Characteristics for Corresponding Damper Failure Case

	1st bending						2nd bending modes			
	Yaw		Roll		Torsion					
Case #	freq. (Hz)	damping	freq. (Hz)	damping	freq. (Hz)	damping	freq. (Hz)	damping	freq. (Hz)	damping
1	0.096	0.146	0.127	0.176	0.188	0.105	0.851	0.01	0.845	0.061
2	0.087	0.284	0.116	0.117	0.188	0.106	0.852	0.010	0.837	0.080
3	0.087	0.285	0.116	0.117	0.188	0.106	0.852	0.010	0.837	0.080
4	0.087	0.285	0.116	0.117	0.188	0.106	0.852	0.010	0.837	0.080
5	0.070	0.184	0.116	0.052	0.188	0.107	0.852	0.013	0.804	0.131
6	0.070	0.184	0.116	0.052	0.188	0.107	0.852	0.013	0.804	0.131
7	0.070	0.184	0.116	0.052	0.188	0.107	0.852	0.013	0.804	0.131
8	0.096	0.147	0.126	0.158	0.169	0.006	0.879	0.011	0.852	0.030
9	0.087	0.285	0.116	0.103	0.169	0.004	0.875	0.008	0.850	0.053
10	0.087	0.285	0.116	0.103	0.169	0.004	0.876	0.008	0.849	0.053
11	0.087	0.285	0.116	0.103	0.169	0.004	0.876	0.008	0.849	0.053
12	0.070	0.184	0.115	0.044	0.169	0.005	0.874	0.005	0.821	0.106
13	0.070	0.184	0.115	0.044	0.169	0.005	0.874	0.005	0.820	0.106
14	0.070	0.184	0.115	0.044	0.169	0.005	0.874	0.005	0.820	0.106
15	0.095	0.005	0.144	0.005	0.203	0.005	0.848	0.005	0.838	0.005
16	0.096	0.149	0.129	0.163	0.203	0.005	0.846	0.005	0.835	0.004
16a	0.066	0.005	0.116	0.005	0.203	0.005	0.846	0.005	0.652	0.005
17	0.095	0.005	0.144	0.010	0.187	0.103	0.852	0.030	0.848	0.005
18	0.066	0.005	0.115	0.005	0.169	0.005	0.873	0.005	0.670	0.005
19	0.095	0.005	0.141	0.005	0.171	0.005	0.889	0.005	0.848	0.005
20	0.087	0.283	0.118	0.112	0.203	0.005	0.846	0.004	0.829	0.062
21	0.087	0.283	0.118	0.112	0.203	0.005	0.846	0.004	0.829	0.062
22	0.087	0.283	0.118	0.112	0.203	0.005	0.846	0.004	0.829	0.062
23	0.07	0.183	0.117	0.0472	0.203	0.005	0.846	0.005	0.797	0.113
24	0.07	0.183	0.117	0.0472	0.203	0.005	0.846	0.005	0.797	0.113
25	0.07	0.183	0.117	0.0472	0.203	0.005	0.846	0.005	0.797	0.113
26	0.066	0.005	0.116	0.005	0.203	0.005	0.846	0.005	0.652	0.005
27	0.066	0.005	0.116	0.006	0.188	0.107	0.852	0.01	0.655	0.009